Journal of
Materials Chemistry A

Accepted Manuscript

This is an *Accepted Manuscript*, which has been through the RSC Publishing peer review process and has been accepted for publication.

Accepted Manuscripts are published online shortly after acceptance, which is prior to technical editing, formatting and proof reading. This free service from RSC Publishing allows authors to make their results available to the community, in citable form, before publication of the edited article. This *Accepted Manuscript* will be replaced by the edited and formatted *Advance Article* as soon as this is available.

To cite this manuscript please use its permanent Digital Object Identifier (DOI®), which is identical for all formats of publication.

More information about *Accepted Manuscripts* can be found in the **Information for Authors**.

Please note that technical editing may introduce minor changes to the text and/or graphics contained in the manuscript submitted by the author(s) which may alter content, and that the standard **Terms & Conditions** and the **ethical guidelines** that apply to the journal are still applicable. In no event shall the RSC be held responsible for any errors or omissions in these *Accepted Manuscript* manuscripts or any consequences arising from the use of any information contained in them.

Mechanism of aluminium incorporation in C-S-H from ab initio calculations†

Luís Pegado,*[a] Christophe Labbez,[b] and Sergey V. Churakov[a]

Received Xth XXXXXXXXXX 20XX, Accepted Xth XXXXXXXXX 20XX
First published on the web Xth XXXXXXXXXX 200X
DOI: 10.1039/b000000x

Blended cements have a big potential to reduce the CO_2 footprint due to cement production. C(alcium)-S(ilicate)-H(ydrate) in these novel materials is known to incorporate a considerable amount of Al. We have for the first time applied large-scale first principles calculations to address the mechanism of Al incorporation in low C/S ratio C-S-H. In agreement with state-of-the-art NMR information, our calculations show that Al substitutes Si in bridging tetrahedra only, and that substitutions in pairing tetrahedra are strongly disfavoured in a wide range of conditions. In broad terms, the energy penalty for having an Al atom in a pairing position is of about 20 Kcal/mol. Al in bridging tetrahedra is therefore the thermodynamically favoured state, rather than merely a kinetically traped one in a solid-liquid equilibrium known experimentally to be very long to reach. A systematic investigation of Al-Al and Defect-Al correlations shows that having two Al atoms as next-neighbours is particularly unfavourable, which gives clues on the limit of Al incorporation in C-S-H. All in all, the current work supports the model and methodology employed to pursue further studies in such materials (e.g., higher C/S ratio systems), in the context of what is still the open question of the structure of C-S-H.

1 Introduction

Concrete, a mix of Portland cement, aggregates and water, is the most commonly used material worldwide. Its production is estimated to be one cubic meter per person per year! This impressive number is explained by its good mechanical properties and ease of use, as well as by the low cost and omnipresence of its constituents, which happen to be the main elements of the earth's crust (Si, Ca, O). However, the production of Portland cement, made from heating to high temperatures ($\sim$1500°C) a mixture of limestones and clays, is responsible for about 5-10% of the global anthropogenic emissions of CO_2 [1–4]. Although considerable research is devoted to new geopolymers as replacements for Portland cement [5], not less attention is dedicated to more eco-friendly and novel cementitious materials [6], i.e. blended cements. In the latter, the main idea is to replace part, if not all, of the limestones which, when calcinated, are responsible for 60% of the carbon footprint of cement ($CaCO_3 \rightarrow CaO + CO_2$).

A recent success is the development of blended fly ash cements produced with considerably less limestones and presenting a low calcium to silicon ratio (C/S). A significant impediment for a wide usage of new cementititious materials, however, is the lack of solid knowledge on their stability and durability. In other words, the equilibrium properties of hydration products in novel cementitious materials are not well-known. Calcium aluminium silicate hydrates (C-A-S-H) are among them.

C-S-H is the main component of hydrated Portland cement paste, and is responsible for the setting and hardening of cement, mainly due to electrostatic, short-range attractive forces between platelets of nanometric dimensions [7–10]. C-S-H nanohydrates form during the hydration of the anhydrous cement grains at their surfaces, following a heterogeneous germination and growth process [11–16].

At low C/S ratio C-S-H has a structure similar to that of a naturally occuring mineral: tobermorite. The main structural elements are a calcium layer flanked on both sides by linear silicate (so-called) dreierketten chains, the latter being formed by alternating bridging and pairing tetrahedra. Al is believed to incorporate calcium silicate hydrates by substituting for Si in these dreierketten chains. Variation of the C/S ratio in C-S-H can happen in two ways: depolimerization of the Si chains through the removal of bridging tetrahedra (i.e., creation of more defects), and adsorption of Ca atoms. The latter charge-compensate the negative surface charges due to the deprotonation of silanol groups. In fact, with increasing pH both the C/S ratio and the surface charge of C-S-H increase [17,18]. On the other hand, the higher the C/S ratio the less Al is incorporated in C-S-H [19], and for C/S ratio above 1.2 the maximum

† Electronic Supplementary Information (ESI) available: see list following the acknowledgements. See DOI: 10.1039/b000000x/

[a] *Laboratory for Waste Management, Paul Scherrer Institute, 5232 Villigen PSI, Switzerland. Fax: 0041 56 310 2821; Tel: 0041 56 310 5757; E-mail: luis.pegado@psi.ch*
[b] *ICB, UMR 6303 CNRS, Université de Bourgogne, F-21078 Dijon Cedex, France.*

Al/Si is under 0.05[20].

Elemental analysis[21–23] performed on blended fly ash cements shows a reduction in C/S ratio in C-S-H, as compared to ordinary Portland cement ("typical" C/S $\simeq$ 1.7), as well as an important Al incorporation (up to about 0.15 Al/Si ratio). Furthermore, solid-state NMR measurements on pure C-A-S-H phase for low C/S ratio (say, 0.7) reveal that most of the aluminium incorporated in C-S-H has a tetrahedral environment and takes the position of the bridging silicates[24–27]. However, it has also been shown[19] that a true equilibrium between the solid (C-A-S-H) and liquid (electrolyte solution of hydroxyde, aluminate, calcium and silicate ions) phases takes extremely long to reach and has so far not been observed. Consequently, the stability of the C-A-S-H phase is still an open question. In particular, one can legitimately ask if the observed substitution of Si with Al in the bridging positions is a kinetically favored state but not the thermodynamically stable one. In other words, can an aluminium substitution in the pairing position be more stable?

Only a few theoretical studies have focused on the Al substitution in C-S-H. Manzano *et al.*[28] have performed DFT stability studies of aluminosilicate dreierketten chains in vacuum, ranging from 1 to 9 Si atoms in length and having at most one Al substitution. In particular, they have rationalized why chains with lengths of 2, 5, 8 ... (3n-1) are more stable than the others. They have also considered environmental effects at the COSMO level, having an effective dielectric constant to mimic the effects of (water) solvation. It was concluded that, for the properties analyzed, the use gas phase calculations was justified. Already some years ago Faucon et al.[29] performed classical molecular dynamics simulations of C-S-H-like structures, using tobermorite as a model. For a C/S ratio of 0.83 they investigated a system with two Al substitutions in bridging sites, and one with one Al in a bridging and one in a pairing positions. For the latter, silicate chain ruptures were observed, which were attributed to the mechanism for charge compensation of the Al substitution. It was concluded that Al should preferentially be in bridging sites. No energetics or relative stabilities of structures were reported. Recently Qomi et al.[30], also based on work with classical potentials, reported free energy differences between an Al substitution in a bridging and in a pairing sites for C-S-H models of different C/S ratio. The general conclusion was that bridging substitutions were always more favourable but by exactly how much was highly dependent on C/S ratio and other particular structural details.

In the current work we employ for the first time large scale first principles calculations to analyze the Al substitution in a large C-S-H lamella, with a particular focus on determining the more stable aluminium location in C-A-S-H. Thanks to the size of the system studied, our calculations also help to understand the spacial correlations between Al substitutions, and between an Al substitution and a surface defect, which can be seen as one of the key factors to explain the limitation of the aluminium incorporation in C-S-H. Using this fundamental understanding we are able to rationalize the experimental observations on C-A-S-H at low C/S ratio and low pH.

2 Models and methods

2.1 C-S-H

C-S-H has been modeled as a single plate, as illustrated in Figure 1 already for a case with two modifications (defects and Al substitutions). The orthorhombic unit cell which generates the original, unmodified plate by translations along the "*a*" and "*b*" cell parameters alone was isolated from the crystal structure of normal 11 Å tobermorite[31]. In doing so one removes all interlayer water and Ca atoms and keeps a single sheet with infinite dreierketten chains of tetrahedrally coordinated silicon atoms on both sides of the central Ca layer. After placement of the protons needed to attain neutral formal charge the unit cell formula reads $2\times(Ca_4Si_6O_{14}(OH)_4\cdot 2H_2O)$. The cell parameters employed were those for 14 Å tobermorite, "*a*"=11.26 (2×5.63) and "*b*"=7.28 (2×3.64)[32]. Note that as long as one is considering a single plate (as opposed to stacks of plates) the structure of 9, 11 and 14 Å tobermorite is the same.

2.2 Aluminium substituted C-S-H (C-A-S-H)

In this study we have investigated C-S-H structures with single and double aluminium substitutions, as well as structures with defects (removed bridging tetrahedra) and single Al substitutions. Figure 1 introduces a simplified representation for our systems, based on depicting only the silicate dreierketten chains on the (upper) surface of our plate, and their changes with respect to the base tobermorite structure. This representation is used in Figure 2 to illustrate four types of Al substitutions studied: in a bridging position (BRIDGE), in a pairing position (PAIR), in the end of a chain (EOC) and in a dimer (formed by two "isolated" pairing tetrahedra between two defects) (DIMER). These constitute particular cases of different environments for a single Al substitution, and are therefore singled-out.

In order to investigate possible correlations between either two Al substitutions, or one defect and one aluminium substitution, an extensive, systematic set of systems has been studied. Here we wish mainly to emphasize that cases are covered where the second of the two modifications to the base tobermorite plate is done in the same silicate dreierketten chain, in the next-neighbour or in the next-next-neighbour compared to the first one, and for varying Al-Al or Al-Defect distances. These systems will be referred to using a matrix-based notation (see Figure 1). We use B, P and D for an Al substitu-

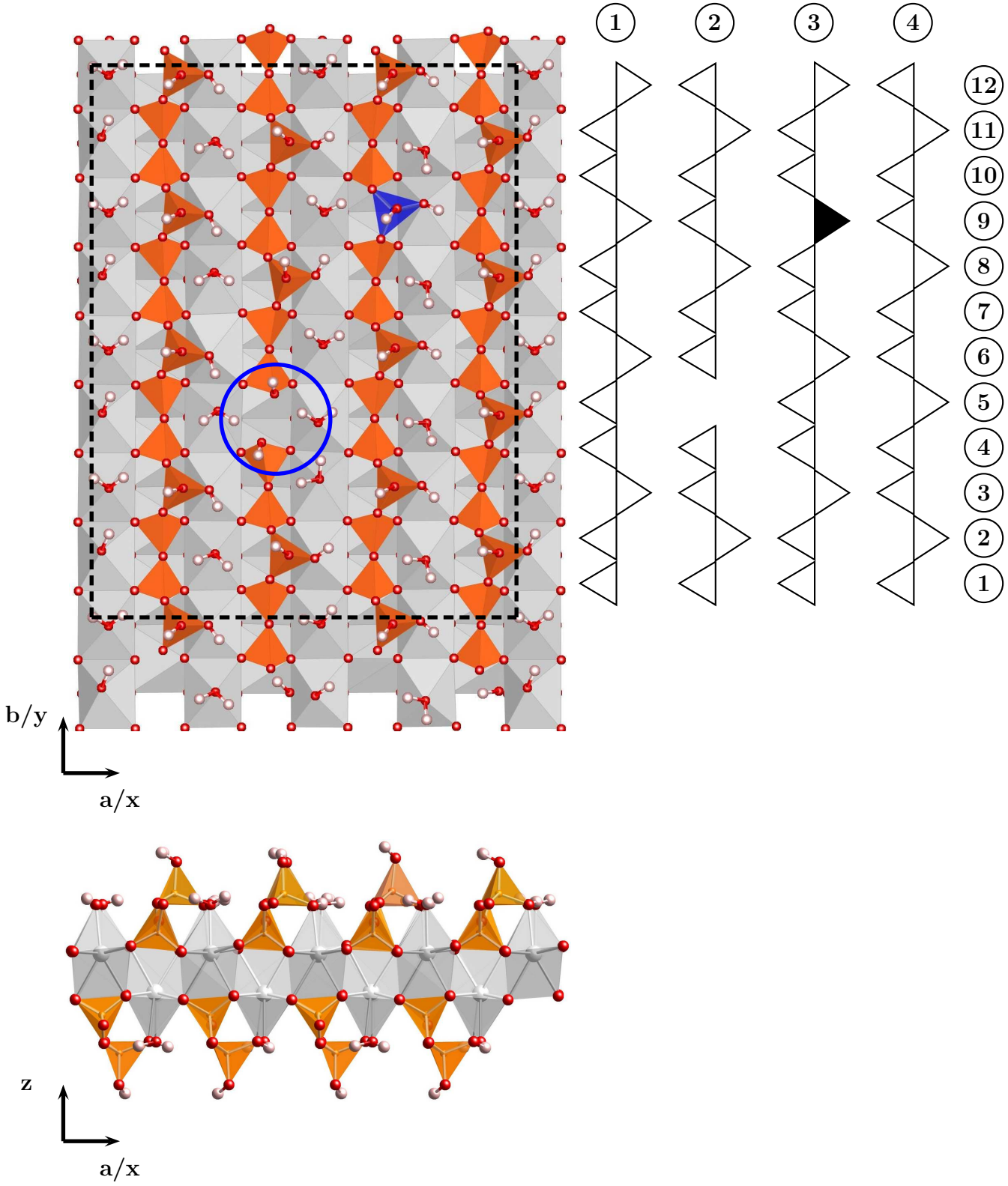

Fig. 1 Caption in the next page.

Fig. 1 (Previous page) The C-S-H model employed in the current work. On the left-hand-side one has two views on the molecular representation of a system already with one defect (D, located within the blue circle) and an Al substitution in a bridging (B) tetrahedron (in blue). Ca atoms are depicted as grey octahedra, Si atoms as yellow tetrahedra, O atoms in red and H atoms in white. The representation is simplified on the right-hand-side by showing only silicate dreierketten chains on the upper part of the plate in a triangle notation, where pairing tetrahedra are triangles pointing left and bridging tetrahedra those pointing right. The filled triangle represents the Al substitution. The column and row numbers (respectively dreierketten chain and tetrahedron number within a dreierketten chain) will be used for a systematic naming of the different systems with two modifications (see text for more details). The system presented is referred to as $D_{2,5}B_{3,9}$. The dashed rectangle isolates the supercell used in our calculations. Note that due to the use of periodic boundary conditions there are no edges and the plate is infinite along the surface directions, x and y.

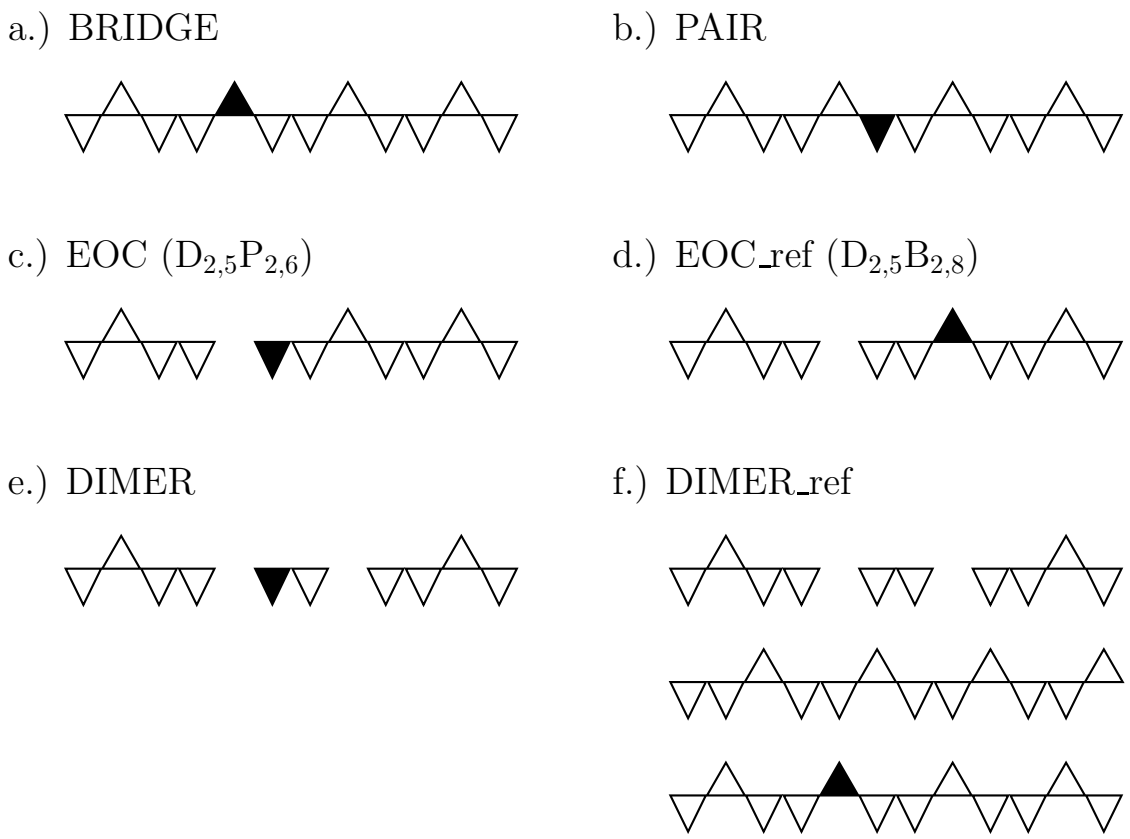

Fig. 2 Schematic representation of a system containing an Al atom in: a.) a bridging position; b.) a pairing position; c.) in the end of a silicate dreierketten chain and e.) in a dimer. Structures d.) and f.) are "reference" structures for, respectively, c.) and e.). They have the same compostion as their corresponding system (same number of defects and Al atoms) but the Al is in a bridging, rather than a pairing position, and are needed for energy difference calculations in Table 1. Non-modified dreierketten chains are in general not shown. For molecular representations of the systems see the SI. The EOC structures are actually particular cases of a series with one Al and one defect, and their designation in our systematic nomenclature system (see Figure 1 and the text) is also given.

tion in a bridging tetrahedron, an Al substitution in a pairing tetrahedron or a defect, respectively. Each letter carries two numerical indices, the first referring to the dreierketten chain ("column") and the second to the tetrahedron number ("row") where each modification occurs. Five series of systems have been explored, namely BB, BP, PP, DB and DP. For molecular representations of all the structures see the SI. The description of the rationale employed when generating the different systems can also be found there. Note that in this work no correlations between Al substitutions or defects across the Ca layer have been considered, only on one of the halves of the plate.

2.3 Calculation details

The geometry of all structures was optimized at the Density Functional Theory level. A multi-step optimization procedure, described in detail in the SI, was followed. All calculations employed the QUICKSTEP module[33] in the CP2K program package[34], version 2.2.426. The Becke exchange[35] and Lee-Yang-Parr[36] correlation functionals have been employed, together with the dispersion correction due to Grimme[37] (BLYP-D2). Goedecker-Teter-Hutter dual-space, norm-conserving pseudopotentials[38] have been used to represent core electrons, and for valence electrons one employed double-ζ, valence polarized, "short-range" MOLOPT basis sets[39] (DZVP-MOLOPT-SR). The electron density was represented in an auxiliary basis set of plane waves up to a cutoff of 320 Ry. On each geometry optimization step the energy was converged to within 1.6×10^{-10} au/atom using a single k-point in the origin of the Brillouin zone (Γ-point sampling). The computational setup employed shares similarities with recent studies of the acidity of hydroxide groups at solid-liquid interfaces (e.g. silica, clays)[40,41] based on *ab initio* molecular dynamics simulations in condensed phase.

The orthorhombic supercell used in our calculations, displayed in Figure 1 (see also the molecular representations in the SI), is obtained by replicating the unit cell described above twice along "*a*" ("x direction") and four times along "*b*" ("y direction"). The system comprises 608 atoms and has x,y,z dimensions of 22.52, 29.12, 25.0 Å. The calculations are periodic in all 3 directions, but the vacuum space left perpendicular to the plate's surface ensures the necessary separation between the different replicas along z. Each substitution of Si with Al implies the introduction of one negative unit charge in the system. These are compensated for with a uniform, neutralizing background. See the SI for a discussion of system size convergence tests performed and also for the comparison of different methods to electrostatically decouple the system from its periodic replicas in the z direction.

Table 1 Energy differences between systems with an Al substitution in a bridging or in a pairing tetrahedron in three different cases. Refer to Figure 2 for system details.

	ΔE / Kcal/mol
PAIR - BRIDGE	17.9
EOC - EOC_ref	18.3
DIMER - DIMER_ref	23.0

3 Results and discussion

Table 1 presents relative energies for systems with a single Al substitution in different environments. Figures 3 and 4 summarize similar data for all systems investigated containing two Al substitutions, or one Al substitution and one defect, respectively. A quick combined analysis unequivocally shows that, for the low C/S ratio systems investigated, an Al substitution in a pairing tetrahedron is always much more unfavourable than in a bridging one.

From Table 1 we see that the energy penalty for having a pairing Al is of the order of 20 Kcal/mol, be it for infinite dreierketten chains, in the end of a chain or even in a dimer (note also the detailed analysis of the two later systems presented in the SI, related to the orientation of "intra-defect" H-bonds, and their - possibly big - effects on the energy). One therefore does not expect to find Al in pairing positions for C-A-S-H at low C/S ratio, which is in full agreement with the best experimental information available[27].

The picture is essentially the same when one has two Al substitutions in the system, or further configurations for one Al and one defect. In Figure 3 the BB, BP and PP sets form series with a scatter of some 10 Kcal/mol, "centered" at 5, 25 and 45 Kcal/mol, respectively (one has excluded from this analysis the innermost point for BP and PP, see below). Two "bands" separated by some 20 Kcal/mol can also be seen in Figure 4 ‡. This analysis also provides our estimate for the uncertainties of the calculations as some 5 Kcal/mol (i.e., half the band width); energy differences smaller than this are not attributed to more than a necessary spread in the results due to the number of degrees of freedom of the system. In the SI further comments are given on what are considered non-determining changes in the energy, due to, e.g., the non-equivalence of two adjacent pairing positions (when the lower half of the unmodified tobermorite plate is considered) or the presence of "intra-defect" H-bonds.

The BP and PP curves in Figure 3 show a particularly strong (anti)-correlation between next-neighbour Al atoms (the point for shortest Al-Al distance in each curve, the $B_{2,5}P_{2,6}$ and

‡ Note that as discussed in the SI some of the systems plotted here have an intra-defect H bond, while others not; still, the reoptimization of all systems with an intra-defect H bond enforced would not change the global picture or our conclusions and was therefore not deemed necessary

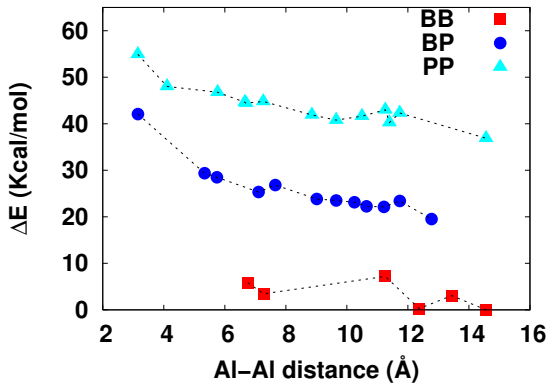

Fig. 3 Relative energies of all the systems with two Al substitutions studied, as a function of Al-Al distance. BB stands for two Al in bridging positions, PP for two Al in pairing positions and BP for one Al in a bridging and one in a pairing position. All energies are referred to the one of the most stable case, $B_{2,5}B_{2,11}$. Refer to the text, Figure 1 and mainly to the SI for more details on the different systems and for the assignment of points to the structures they correspond to.

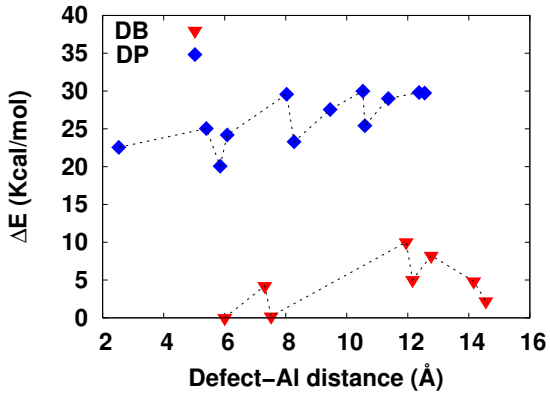

Fig. 4 Relative energies of all the systems with one defect and one Al substitution studied, as a function of Defect-Al distance. DB stands for one defect and one Al in a bridging position and DP for one defect and one Al in a pairing position. The Defect-Al distances were measured using for all systems the same point as location of the defect, as explained in the SI. All energies are referred to the one of the most stable system, $D_{2,5}B_{1,6}$. Refer to the text and to the SI for more details on the different structures.

$P_{2,6}P_{2,7}$ systems, respectively). For large separations one expects the relative energy profiles to plateau. Within our previously defined error bars this is indeed what is happening. We note that the three curves displayed have in broad terms a similar distance dependence and, in fact, the strong avoidance of next-neighbour Al atoms could be the explanation for the limit of Al incorporation in C-S-H of about 0.15 (in Al/Si ratio). As far as Figure 4 goes, no appreciable correlations are seen in the relative positions of Al atoms and defects in the system. We stress that in Figures 3 and 4 one has structures with 2 modifications (Al substitution or defect) in the same, next-neighbour or next-next neighbour silicate chains. However, a closer look at the data (using the correspondence between points and systems in the SI) does not reveal any particular characteristic in any sub-series, and the Al-Al (or Defect-Al) distance seems in fact to be the most important parameter.

Manzano *et al.*[28] have reported that for a pentameric silicate chain in vacuum having the Al in the end of the chain is energetically less favourable than having it in the bridging position by about 21 Kcal/mol. However, having an Al in the pairing position adjacent to the bridging one was only less favourable by 4 Kcal/mol, in clear constrast with our results. In particular, our two "pairing systems" directly comparable to those of Manzano and co-workers, $D_{2,5}P_{2,6}$ and $D_{2,5}P_{2,7}$, differ in energy only by approximately 2.5 Kcal/mol, being above the reference system for Figure 4 by respectively 22.5 and 25 Kcal/mol (section 7 of the SI). One is therefore led to conclude that the further elements included in our model, in particular the presence of the Ca layer and/or the vicinity of other silicate chains is decisive in rendering any pairing position equally unfavourable.

The comparison with Qomi *et al.*'s work with classical potentials[30] is not always so clear cut. The differences in (room temperature) free energies reported were obtained from lattice dynamics energy minimization within the harmonic approximation. For a C-S-H model with C/S ratio of 0.66 (that of our unmodified tobermorite plate) the difference between having an Al in a bridging versus in a pairing position is of 11.5 Kcal/mol, reasonably close to what we have reported here. However, when the C/S ratio rises to 0.83 the difference is of 111 Kcal/mol. The C/S ratio was increased by putting Ca atoms in the interlayer space between two tobermorite plates. Besides this, the two systems also differ in interlayer space (11 and 14 Å tobermorite structures were used for respectively 0.66 and 0.83 C/S) and in the fact that for 0.66 C/S ratio the chains of opposing plates are "fused" through the tips of bridging tetrahedra (forming so-called double dreierketten chains). In both cases, however, the chains are defect-free. One can also add that for a structure with C/S ratio higher than 1 (finite dreierketten chains) the substitution in the pairing tetrahedron in the end of a pentameric chain, and in the adjacent pairing position, are higher in energy than the bridging substitution by respectively 434 and 300 Kcal/mol. Our first principles results indicate more modest energy differences, even if also way above the thermal energy at room temperature.

It is important to mention that experimental evidence of Al incorporation in what are believed to be pairing positions has also been reported[27]. This happens however for C-A-S-H at

higher C/S ratio (above 0.95) and higher pH. The appearence of Al in pairing tetrahedra at high C/S ratio has also been suggested based on classical molecular dynamics simulations[42]. This type of systems is outside the scope of the current contribution, which has however paved the way for such investigations. As already mentioned the increase of the C/S ratio in C-S-H can happen both through depolimerization of the Si chains and adsorption of Ca atoms. It is likely that this second mechanism will be of importance when modelling materials at high C/S, in particular when one thinks that the current studies have pointed to a lack of correlation between the positions of defects and Al atoms, at least for fully protonated surfaces.

4 Conclusion

The current study addressed the still open question of the long-term stability of C-A-S-H phases in cementitious materials. The *ab initio* calculations performed are in full agreement with state-of-the-art NMR experiments on low pH/low C/S ratio systems. They strongly indicate that, under such conditions, Si substitution by Al in bridging positions is in fact the thermodynamically most favourable. For all configurations with Al in a pairing position the energy penalty was of the order of 20 Kcal/mol. This makes such configurations thermodynamically unfavourable.

Despite decades of research, the structure of C-S-H is not yet fully established. The current study also serves the purpose of assessing the value of tobermorite as a model system, and of the computational setup employed. We have put the emphasis on performing a systematic study of different aspects of Al substitution under relatively simple, yet realistic and relevant conditions. One can now build up on this to increase the complexity step-wise and study further problems in such a challenging system as C-S-H can be. Besides (pairing) substitutions for higher C/S ratio, another issue of interest are the penta and hexacoordinated Al species which are supposed to appear on the sides of C-A-S-H. These questions will involve looking at the tobermorite interlayer space and also at edges.

Further steps towards an accurate estimation of the thermodynamics of Al incorporation in C-S-H would be to include the effect of surface hydration. The Al-Si exchange free energy could be obtained by thermodynamic integration based on molecular dynamics simulations. This will be the focus of a follow-up study.

Acknowledgements

L.P. acknowledges financial support by the SNF, Switzerland, under grant number CRSI22_130419/1. The use of computer resources at the Merlin 4 cluster, Paul Scherrer Institute, Switzerland and at the Swiss National Center for Scientific Computing (CSCS, Lugano) are also gratefully acknowledged. The authors also thank André Nonat for many enlightening discussions on C-(A)-S-H.

Supplementary Information Available

In a single PDF file the following are provided:

- 1.) description of the rationale for generating the systems with 2 Al substitutions or 1 Al and one defect
- 2.) molecular representations of the systems in Figure 2
- 3.) molecular representations of the systems for Figure 3
- 4.) molecular representations of the systems for Figure 4
- 5.) details of the geometry optimization strategy
- 6.) details on size convergence and electrostatic decoupling tests
- 7.) the data for Figures 3 and 4
- 8.) explanation of how Defect-Al distances for Figure 4 were calculated
- 9.) a few further notes on ”error bars”
- 10.) description of the effect of starting proton configurations for the DIMER systems

Furthermore, coordinate files (XYZ) for all the systems mentioned in points 2, 3, 4, 6, 8, 9 and 10 above are provided, with the same name as used in the text of the PDF file.

References

1 J. N. Hacker, T. P. D. Saulles, A. J. Minson and M. J. Holmes, *Energy Build.*, 2008, **40**, 375.
2 G. P. Harrison, E. J. Maclean, S. Karamanlis and L. F. Ochoa, *Energy Policy*, 2010, **38**, 3622.
3 P. Purnell, *Environ. Sci. Technol.*, 2012, **46**, 454.
4 I. Amato, *Nature*, 2013, **494**, 300.
5 J. L. Provis, G. C. Lukey and J. S. J. van Deventer, *Chem. Mater.*, 2005, **17**, 3075.
6 E. Durgun, H. Manzano, R. J. M. Pellenq and J. C. Grossman, *Chem. Mater.*, 2012, **24**, 1262.
7 R. J. M. Pellenq, J. Caillol and A. Delville, *J. Phys. Chem. B*, 1997, **101**, 8584.
8 A. Delville, R. J. M. Pellenq and J. Caillol, *J. Chem. Phys.*, 1997, **106**, 7275.
9 H. van Damme, in *Encyclopedia of Surface and Colloid Science*, Marcel Dekker: New York, 2002, p. 1087.
10 B. Jönsson, A. Nonat, C. Labbez, B. Cabane and H. Wennerström, *Langmuir*, 2005, **21**, 9211.
11 H. F. W. Taylor, *Cement Chemistry*, Academic Press Ltd.: London, 1990.
12 S. A. FitzGerald, D. A. Neumann and J. J. Rush, *Chem. Mater.*, 1998, **10**, 397.

13 J. J. Thomas and H. M. Jennings, *Chem. Mater.*, 1999, **11**, 1907.
14 S. Garrault and A. Nonat, *Langmuir*, 2001, **17**, 8131.
15 V. K. Peterson and M. C. G. Juenger, *Chem. Mater.*, 2006, **18**, 5798.
16 J. W. Bullard, H. M. Jennings, R. A. Livingston, A. Nonat, G. W. Scherer, J. S. Schweitzer, K. L. Scrivener and J. J. Thomas, *Cem. Concr. Res.*, 2011, **41**, 1208.
17 A. Nonat, *Cem. Concr. Res.*, 2004, **34**, 1521.
18 C. Labbez, I. Pochard, B. Jönsson and A. Nonat, *Cem. Concr. Res.*, 2011, **41**, 161.
19 X. Pardal, I. Pochard and A. Nonat, *Cem. Concr. Res.*, 2009, **39**, 637.
20 X. Chen, *PhD thesis*, Université de Bourgogne, 2007.
21 T. T. H. Bach, C. C. D. Coumes, I. Pochard, C. Mercier, B. Revel and A. Nonat, *Cem. Concr. Res.*, 2012, **42**, 805.
22 F. Brunet, T. Charpentier, C. N. Chao, H. Peycelon and A. Nonat, *Cem. Concr. Res.*, 2010, **40**, 208.
23 M. Antoni, J. Rossen, F. Martirena and K. Scrivener, *Cem. Concr. Res.*, 2012, **42**, 1579.
24 X. D. Cong and R. J. Kirkpatrick, *Adv. Cem. Bas. Mat.*, 1996, **3**, 144.
25 P. Faucon, T. Charpentier, A. Nonat and J. C. Petit, *J. Am. Chem. Soc.*, 1998, **120**, 12075.
26 M. D. Andersen, H. J. Jakobsen and J. Skibsted, *Inorg. Chem.*, 2003, **42**, 2280.
27 X. Pardal, F. Brunet, T. Charpentier, I. Pochard and A. Nonat, *Inorg. Chem.*, 2012, **51**, 1827.
28 H. Manzano, J. S. Dolado and A. Ayuela, *J. Phys. Chem. B*, 2009, **113**, 2832.
29 P. Faucon, J. M. Delaye, J. Virlet, J. F. Jacquinot and F. Adenot, *Cem. Concr. Res.*, 1997, **27**, 1581.
30 M. J. A. Qomi, F.-J. Ulm and R. J.-M. Pellenq, *J. Am. Ceram. Soc.*, 2012, **95**, 1128.
31 S. Merlino, E. Bonaccorsi and T. Armbruster, *Eur. J. Mineral.*, 2001, **13**, 577.
32 E. Bonaccorsi, S. Merlino and A. R. Kampf, *J. Am. Ceram. Soc.*, 2005, **88**, 505.
33 J. VandeVondele, M. Krack, F. Mohamed, M. Parrinello, T. Chassaing and J. Hutter, *Comput. Phys. Commun.*, 2005, **167**, 103.
34 http://www.cp2k.org.
35 A. D. Becke, *Phys. Rev. A*, 1988, **38**, 3098.
36 C. Lee, W. Yang and R. G. Parr, *Phys. Rev. B*, 1988, **37**, 785.
37 S. Grimme, *Journal of Computational Chemistry*, 2006, **27**, 1787.
38 S. Goedecker, M. Teter and J. Hutter, *Phys. Rev. B*, 1996, **54**, 1703.
39 J. VandeVondele and J. Hutter, *J. Chem. Phys.*, 2007, **127**, 114105.
40 M. Sulpizi, M.-P. Gaigeot and M. Sprik, *J. Chem. Theory Comput.*, 2012, **8**, 1037.
41 S. Tazi, B. Rotenberg, M. Salanne, M. Sprik and M. Sulpizi, *Geochim. Cosmochim. Acta*, 2012, **94**, 1.
42 H. Manzano, J. S. Dolado, M. Griebel and J. Hamaekers, *phys. stat. sol. (a)*, 2008, **205**, 1324.

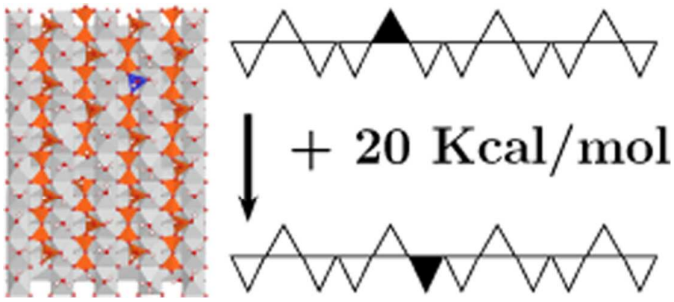

Al substitution in Calcium Silicate Hydrate (C-S-H) in novel, low CO2 cementitious materials takes place in bridging tetrahedral positions only.